Erosion and flexural uplift along transform faults

Christophe Basile, Pascal Allemand

Geophys. J. Int. (2002) **151,** 646–653

Erosion and flexural uplift along transform faults

Christophe Basile[1] and Pascal Allemand[2]

[1]*Laboratoire de Géodynamique des Chaînes Alpines, UMR* 5025, *OSUG, Université Joseph Fourier, Grenoble, France. E-mail: cbasile@ujf-grenoble.fr*
[2]*Laboratoire de Sciences de la Terre, UMR* 5570, *Université Claude Bernard, Villeurbanne, France*

Accepted 2002 July 4. Received 2002 July 4; in original form 2002 March 11

SUMMARY

In all geodynamic settings (intracontinental, continent–ocean, intraoceanic), the main morphological feature of transform plate boundaries is a narrow and elongated valley bounded on at least one side by an uplifted shoulder. Several mechanisms have been proposed to explain this uplift: differential thermal subsidence, lateral heat transfer, extension perpendicular to the transform, but none can be used in all settings. We propose that the erosion of a lithospheric plate along the transform boundary may be an alternative mechanism that can be active in all geodynamic settings. Erosional unloading produces flexural uplift along the transform border, which does not exceed 35–40 per cent of the difference in height between the lithospheric plate and the transform valley. Our model perfectly fits the morphology of several examples in the continental lithosphere: the uplifted shoulder of the Dead Sea transform, as well as marginal ridges in continental transform margins. Along an oceanic transform fault, the erosion of the transform border only partially explains the uplift of the highest transverse ridges, but may amplify other mechanisms.

Key words: continental margins, Dead Sea, flexure of the lithosphere, transform faults, uplift.

INTRODUCTION

Among plate boundaries, transform faults are defined as vertical planes between two lithospheric plates sliding horizontally one against the other. When transform faults connect divergent plate boundaries, a narrow and elongated valley where the seismically active fault is located characterizes their topography. This valley is bounded on at least one side by an asymmetric ridge, with a steep slope towards the transform valley and a gentle slope outwards. This topography is observed in all geodynamic settings: intracontinental transform faults, such as along the Dead Sea rift (Fig. 1a), intraoceanic transform faults (transverse ridges (Fig. 1b), Bonatti 1978) and Fracture Zones (FZ, Sandwell & Schubert 1982), or at the continent–ocean transition (marginal ridges in transform continental margins (Fig. 1c), Basile *et al.* 1993). In every case, the shape of the asymmetric ridge can be described by the upward flexure of the edge of a lithospheric elastic plate. Several hypotheses have been proposed to explain this flexure, mainly related either to the lithospheric thermal behaviour, or to tectonism. Whereas the topography of transform faults appears to be quite uniform, each model can only be used in a specific case.

(1) For intraoceanic FZ, Sandwell & Schubert (1982) proposed that the initial vertical offset at the ridge–transform intersection is locked (i.e. the two lithospheres are coupled across a FZ), and that differential thermal subsidence far from the FZ induces bending in the vicinity of the FZ (Fig. 2a).

(2) For active intraoceanic transform faults, uplift or subsidence has been inferred to result from shear heating and lateral heat conduction across the transform (Chen 1988). These vertical displacements may disappear with time when the transform zone becomes inactive and when thermal equilibrium between the two lithospheres is reached (Fig. 2b).

(3) For transform continental margins, Todd & Keen (1989) proposed a similar model based on shear heating and lateral heat conduction. Crustal uplift is also transient, but can be amplified by erosion and associated local isostatic compensation.

(4) For intracontinental transform faults, no significant differential thermal subsidence or heat transfer is expected. Tectonic mechanisms (mainly extension perpendicular to the transform fault) are the main hypotheses used, for example by Wdowinski & Zilberman (1996) for the Dead Sea Rift (Fig. 2c). Extension has also been proposed in other geodynamic settings when thermal models were clearly inadequate to explain the observed topography (Pockalny *et al.* (1996) for the Kane FZ; Clift & Lorenzo (1999) for the Côte d'Ivoire–Ghana (CIG) transform margin). Other mechanical processes have also been proposed, such as lithospheric flow parallel to the transform along transform continental margins (Reid 1989), or twisting moments exerted along the transform fault at ridge–transform intersections (Chen 1989).

A detailed discussion of this set of hypotheses is beyond the scope of this paper. However, this overview emphasizes the lack of a common model for an almost ubiquitous topography. This paper is based on a simple observation: with the exception of extensional mechanisms, the transform fault is assumed in all models to be a vertical boundary above and below the Earth's surface. However, even if transform fault escarpments are among the steeper slopes

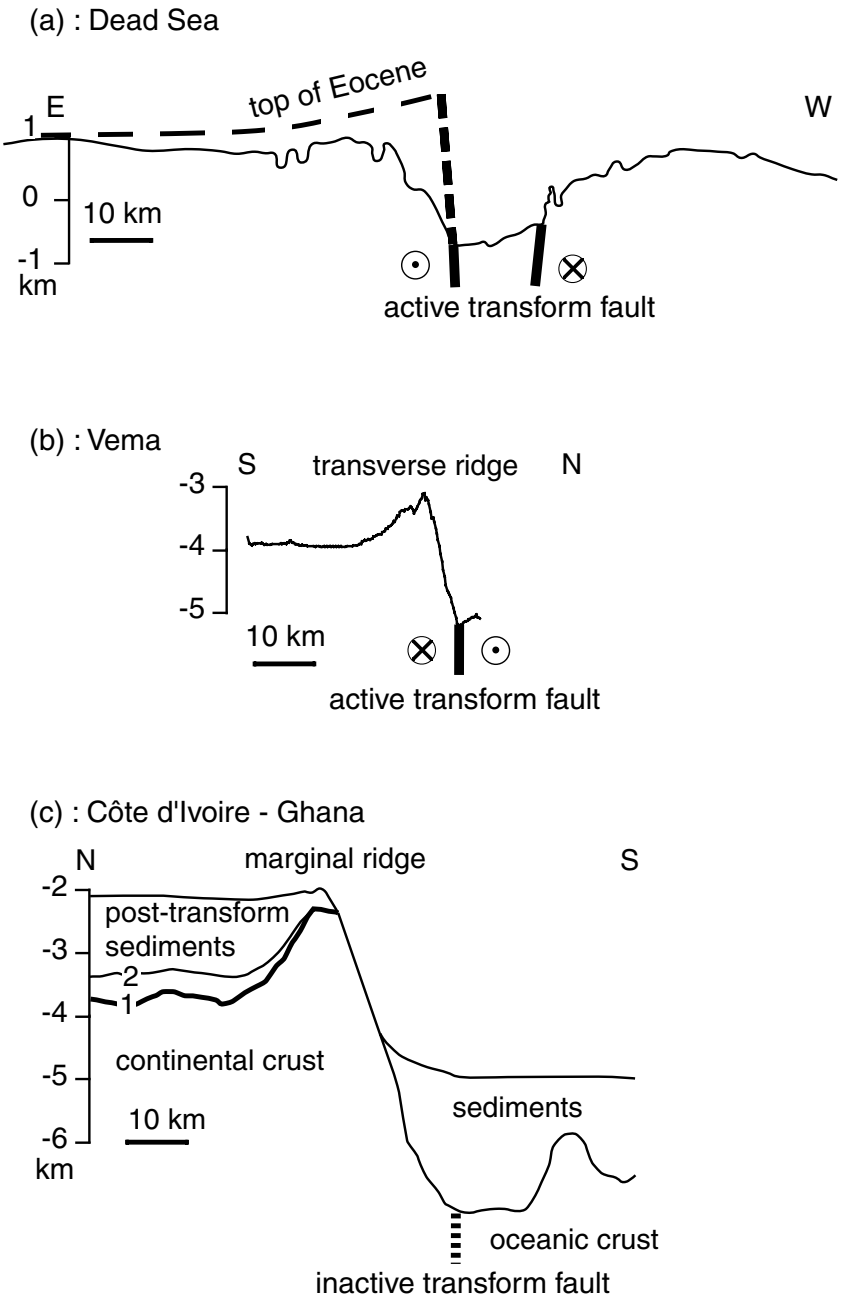

Figure 1. Topographic and bathymetric sections of intracontinental (a, Dead Sea Rift, from Wdowinski & Zilberman 1997), intraoceanic (b, Vema transverse ridge, from InterRidge Data Base), and continent–ocean (c, Côte d'Ivoire–Ghana marginal ridge; 1 top Santonian; 2 top Paleocene) transform faults. Same vertical and horizontal scales for the three sections. Vertical exaggeration $\times 10$.

on the Earth's surface, they are still far from vertical as they are submitted to aerial or submarine erosion. The aim of this paper is to examine the effects of this erosion on the unloading of the transform boundary, and consequently on the topography of transform fault shoulders.

EROSION AND FLEXURAL MODELLING

A vertical transform fault brings into contact two lithospheres characterized by a distinct nature, thickness, thermal structure and/or age. In transform continental margins, the change of thickness from continental to oceanic crust results in a several kilometres high topographic step (e.g. Fig. 1c). In intracontinental or intraoceanic settings, the change of elevation between the two plates on either side of the transform fault is not so great. However, when the transform fault connects a divergent plate boundary, an important step appears again between the lithospheric plate and the deep valley that follows the transform fault (e.g. Fig. 1a for the Dead Sea transform). The origin of this transform valley itself is unclear: it can result from transtension if the plate motion is not always exactly parallel to the transform fault (Cronin 1991); it can also result from extension parallel to the transform fault, as in the numerous pull-apart basins observed along the Dead Sea transform (e.g. Garfunkel *et al.* 1981).

In both cases (lithospheric plate against lithospheric plate, or lithospheric plate against transform valley), the transform fault is

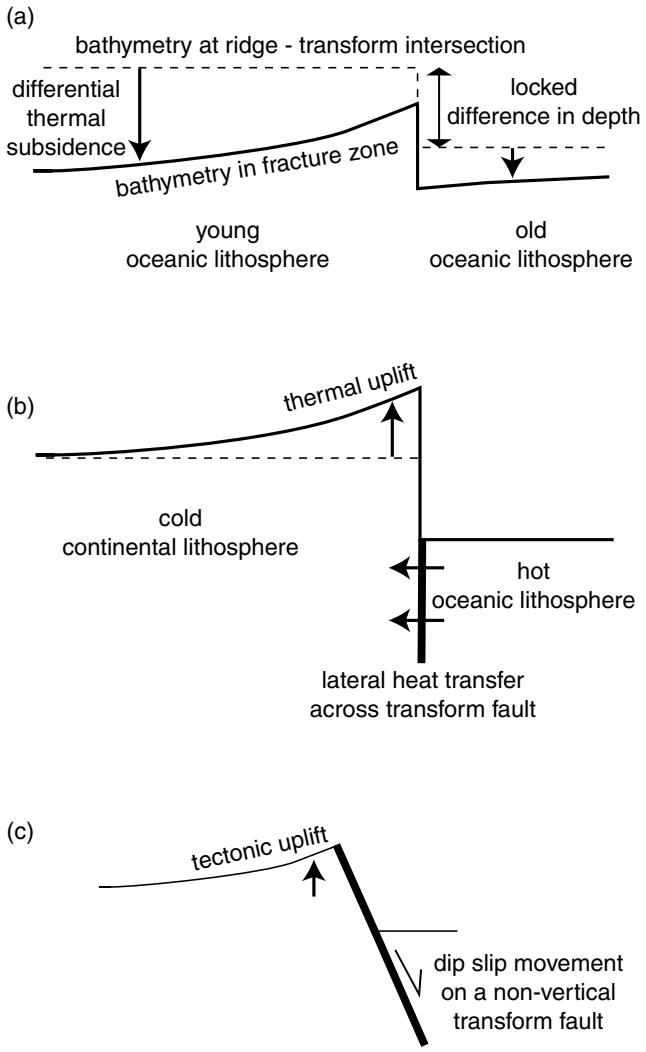

Figure 2. Main mechanisms proposed to explain flexural uplift along transform faults: (a) differential thermal subsidence across a locked transform fault; (b) thermal expansion caused by lateral heat transfer across the transform fault; (c) tectonic extension (and induced unloading) perpendicular to an inclined transform fault.

associated with a topographic step, with distinct surface elevation on each side of the vertical fault (Fig. 3a). As a vertical plane cannot be preserved at the Earth's surface, the higher corner is expected to be eroded by gravitational processes, inducing unloading and uplift by isostatic compensation. The flexural modelling presented in this paper (called hereafter the erosional model) considers only the behaviour of the higher plate assumed to be an elastic plate with elastic thickness h_e, Young's modulus $E = 7 \times 10^{10}$ Pa, Poisson's ratio $\nu = 0.25$ and volumic mass $\rho = 2800$ kg m^{-3}. The equation to be solved is (Turcotte & Schubert 1982):

$$\frac{Ehe^3}{12(1-\nu^2)}\frac{d^4\omega}{dx^4} + (\rho_m - \rho_w)g\omega = q(x) \quad (1)$$

where g is the acceleration due to the gravity, ρ_m is the volumic mass of the mantle (3300 kg m^{-3}), ρ_w is the volumic mass of water (1000 kg m^{-3}) or air (0), ω is the plate deflection and $q(x)$ is the load by unit length. The equation is solved using a finite-difference scheme (e.g. Van Wees 1994) with a mesh of 100 m. The flexure is computed on a section perpendicular to the transform

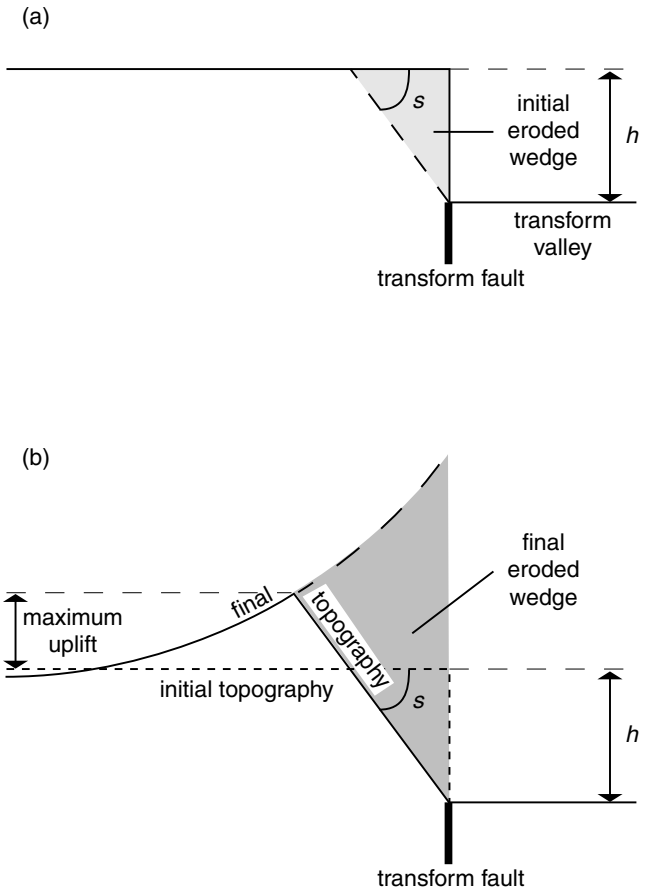

Figure 3. Flexural response of unloading by erosion of a transform border: (a) initial topography; (b) final topography. s erosional slope, h difference of height.

fault. The transform edge of the plate acts as a free border, as it is assumed to be decoupled from the other plate by the vertical transform fault. The unloading is computed from the shape of the wedge of eroded material, which depends on both the erosional slope s and the difference in height h between the two plates (Fig. 3a). Both aerial and submarine erosion (eroded materials being replaced by water) are considered. The erosion is estimated using an iterative process. In a first run, the upper corner of the unloaded plate is eroded to the definite slope s (Fig. 3a). The elastic flexure and a new plate topography are computed. As this new topography has lost the definite slope in the eroded region, additional erosion is applied. The iterations stop when the thickness of the eroded material during a cycle is less than 1 m (Fig. 3b).

A series of calculations varying T_e, s and h have been made to test the effects of these parameters (Fig. 4). The maximum elevation reached by the uplifted plate is always located at the intersection between the erosional slope (toward the transform fault) and the flexural slope, the shape of which is controlled by the elastic thickness (Fig. 4c). The maximum elevation increases with h and follows a sigmoidal curve (Fig. 5). The elevation is small when h is below 0.5–1 km, as the unloading is too small to significantly uplift the plate. There is a rapid increase in maximum elevation for h above 1 km, and an upper limit for high to very high values of h. For a thin elastic plate and a gentle slope (e.g. $T_e = 5$ km and $s = 5^\circ$), the upper limit is rapidly reached. In contrast, for a thick elastic plate and a steep slope (e.g. $T_e > 10$ km and $s > 10^\circ$), the maximum uplift increases slowly with h. Between these two end-members,

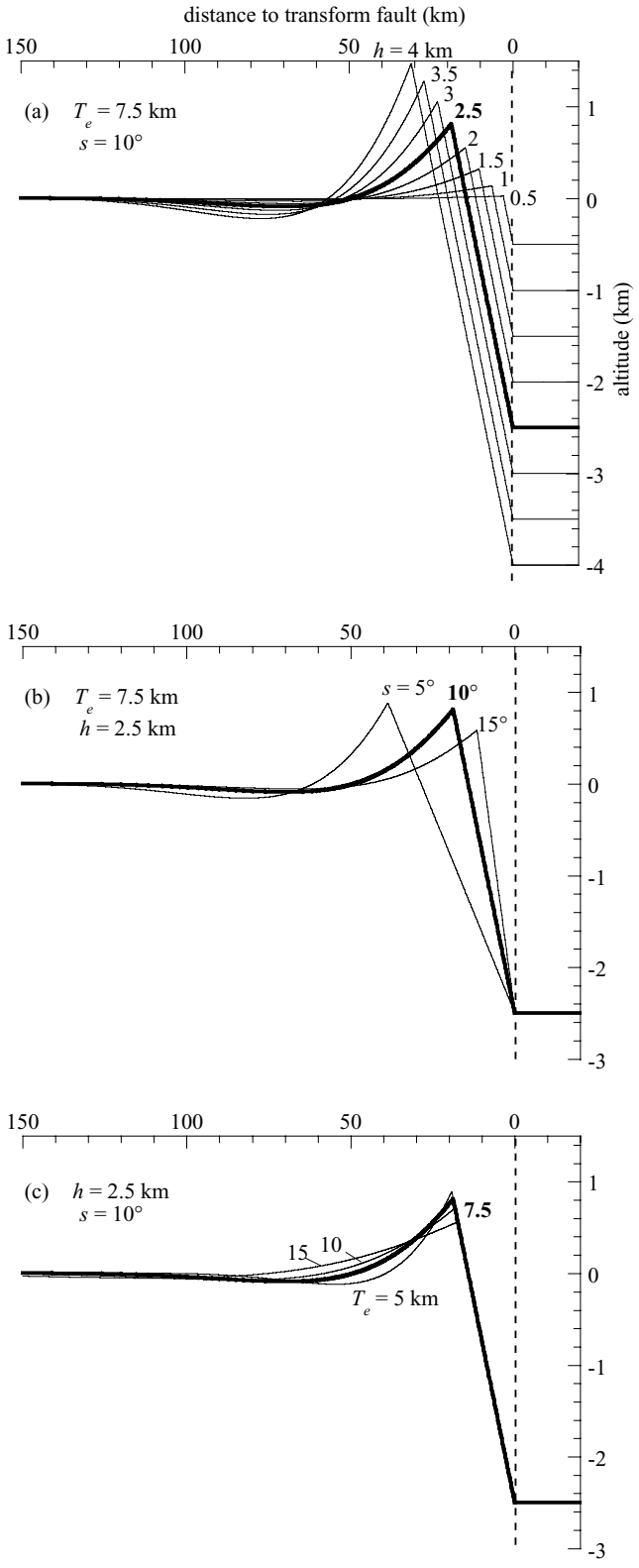

Figure 4. Influence of some parameters (h elevation difference, s erosional slope and T_e elastic thickness, (a)–(c), respectively) on the shape of the flexed plate. All experiments are performed below sea level. Vertical exaggeration ×28. In each figure, the bold line indicates the same experiment (T_e = 7.5 km, h = 2.5 km, s = 10°).

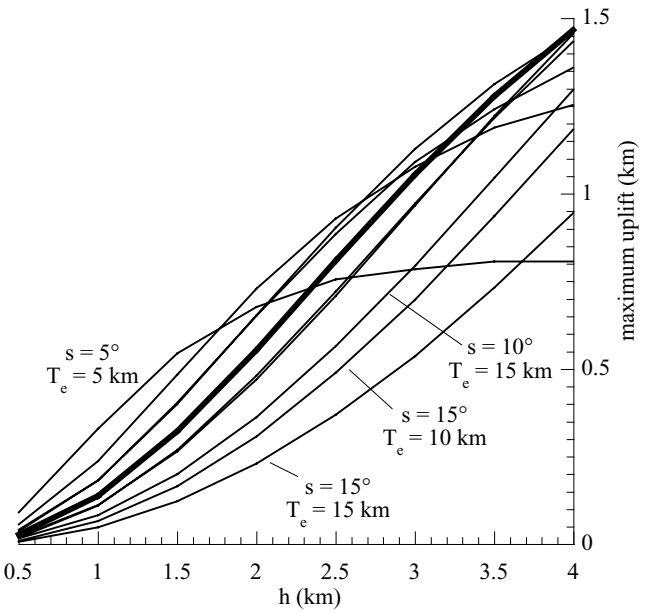

Figure 5. Maximum uplift of the flexed plate. All experiments are performed below sea level. The bold line indicates the maximum uplift for the experiments shown in Fig. 4(a) (T_e = 7.5 km, s = 10°).

the uplift is quite independent of the elastic thickness and erosional slope. In any case, the maximum uplift does not exceed 35 per cent of the difference in height h for submarine transform faults. The maximum uplift is increased by 20 per cent for subaerial cases.

To test the erosional model in several geodynamic settings, we measured the erosional slope s and the vertical topographic offset h between the transform fault (most of the time inside the transform valley) and the adjacent uplifted plate far away from the transform boundary (Fig. 3). The parameter s is then fixed for each model, and h is used as a starting value that can be modified to fit the observed uplift. An appropriate elastic thickness T_e is chosen to fit the shape of the flexural slope. Examples from three geodynamic settings were tested: the Dead Sea transform (intracontinental), the CIG and Senja transform continental margins (continent–ocean), and the Vema and Orozco transform faults (intraoceanic).

DEAD SEA TRANSFORM

The Dead Sea transform is a narrow 500 km long depression following a sinistral transform fault, which offsets the Arabian plate from the eastern Mediterranean plate by 105 km. The eastern side of the transform has the shape of a flexurally uplifted shoulder, especially south of Lake Kineret and south of the Dead Sea, where it forms the Trans-Jordan mountain belt (Wdowinski & Zilberman 1997). In this area, we used the topography of two sections perpendicular to the transform fault to test the erosional model. Each topographic section is representative of a 50 km long segment along the transform. In the northern section (Fig. 6a), the model fits the topography very well, in accordance with the flexural slope, the erosional slope, the difference in height and the location of the transform fault at the bottom of the erosional slope. In the southern section (Fig. 6b), the transform fault is not located at the bottom of the erosional fault, but more or less in the middle of the transform valley (Garfunkel *et al.* 1981). In this example a best fit between the erosional model

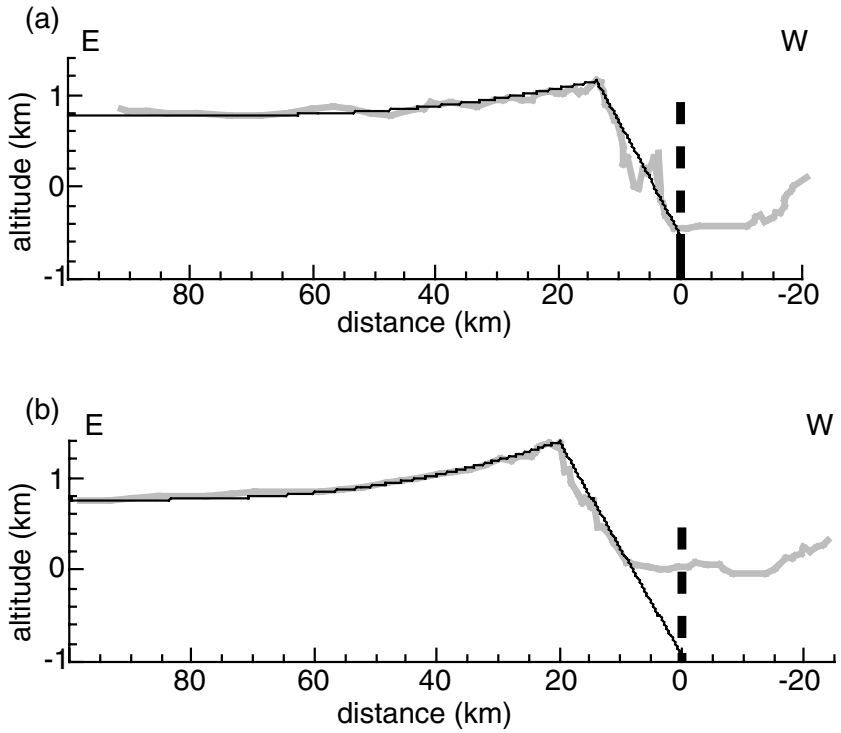

Figure 6. Modelling of the flexure of an elastic plate compared with the topography of the Dead Sea shoulders (from Section 31 (a) and 43 (b) of Wdowinski & Zilberman 1997). Same vertical and horizontal scales, vertical exaggeration ×15. The thin black lines represent the models, the thick grey lines the topography, and the thick vertical lines indicate the transform fault. For (a), $h = 1.32$ km, $T_e = 11$ km, $s = 7°$; for (b), $h = 1.74$ km, $T_e = 12.5$ km, $s = 6.6°$. Both are above sea level.

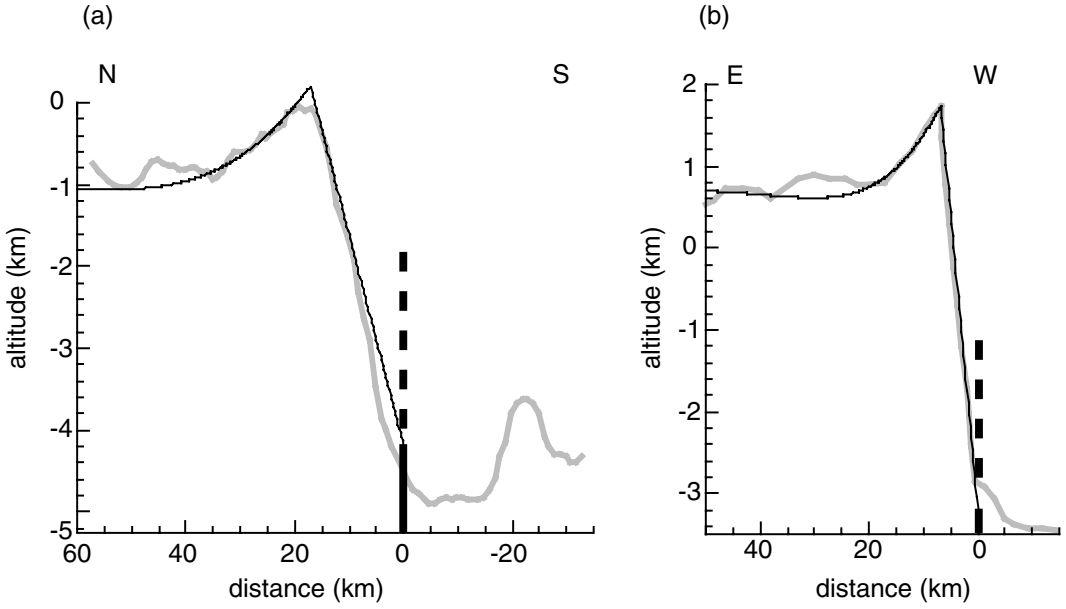

Figure 7. Modelling of the flexure of an elastic plate compared with the topography of marginal ridges of transform continental margins. (a) CIG marginal ridge, reconstructed at Santonian times; $h = 3.26$ km, $T_e = 5$ km, $s = 14.4°$. (b) Senja marginal ridge, reconstructed at Eocene times (from Vågnes 1997); $h = 3.91$ km, $T_e = 2.5$ km, $s = 36°$. Both are below sea level. Same legend as in Fig. 6.

and the topography requires the erosional slope to be extended down to the transform fault, i.e. that the difference in height h has been more important than is observed today, because of sedimentary infilling of the transform valley. However, in both examples, most of the sediments produced by the erosion of the transform border are displaced laterally inside the transform valley, toward the Dead Sea Basin. The estimated thickness of the elastic plate (11–12.5 km) is comparable to the elastic thickness of continental lithospheres with the strength being controlled by the crust (Burov & Diament 1995).

TRANSFORM CONTINENTAL MARGINS

We use two reconstructions of transform continental margins, the first for the CIG transform margin at Santonian times (based on Basile *et al.* 1998), and the second one proposed by Vågnes (1997) for the Senja transform margin at Eocene times. On the northern border of the Gulf of Guinea, the CIG transform margin exhibits a very prominent marginal ridge, 1.5 km high and more than 100 km long. This ridge was uplifted during Cretaceous times, and was then onlapped by sediments. The erosional model is tested on a reconstruction at Santonian times, at the end of transform fault activity, when the oceanic crust was emplaced along the transform margin (Basile *et al.* 1993). This reconstruction is built by unfolding the top of the Paleocene sediments (Fig. 1c), known to be a horizontal surface during deposition (Mascle *et al.* 1996; Basile *et al.* 1998), and decompacting the Santonian–Paleocene interval. The erosional model (Fig. 7a) closely fits with this Santonian reconstruction for all parameters (flexural slope, erosional slope, difference in height and location of the transform fault at the bottom of the erosional slope). The Senja transform margin, in the Norwegian–Greenland Sea, has been reconstructed by Vågnes (1997) at the same stage of evolution, when the oceanic spreading centre passed along the transform margin. Here again, the erosional model fits the reconstructed topography (Fig. 7b). No additional mechanism, such as lateral heat conduction, ductile flow or tectonically driven uplift are required to explain this topography. In both cases the material resulting from the erosion of the transform border may be deposited in the active transform valley, and subsequently deformed by the transform fault. Such sediments derived from the CIG transform margin were encountered far from the continent all along the Romanche FZ (Honnorez *et al.* 1994; Bonatti *et al.* 1996). In both examples, the reduced thickness (5 and 2.5 km) of the elastic plate can be explained by crustal thinning (the crustal thickness is less than 18 km in CIG, Sage *et al.* 2000) and by intense deformation along the transform boundary.

INTRAOCEANIC TRANSFORM

Intraoceanic transform faults represent the largest relief features on the deep seafloor, because of transform troughs, which are deeper than the adjacent oceanic crust, and transverse ridges, which rise above the oceanic crust by several hundreds to thousands of metres. The uplift of most transverse ridges is more than 60 per cent (and often more than 100 per cent) of the difference in depth between the adjacent oceanic crust and the transform trough. As the erosional model allows a maximum uplift of less than 35 per cent in submarine environments, it is clear that this mechanism alone cannot explain the elevation of the high-standing transverse ridges. However, in some places such as the eastern part of the Vema transform fault (Lagabrielle *et al.* 1992), or the Orozco transform fault (Madsen *et al.* 1986), the uplift of the transform border is more limited. In these cases, the erosional model correctly fits the bathymetry (Figs 8a and b). In the Vema transform, the erosion is attested to by a thick sedimentary breccia observed in the transform valley (Lagabrielle *et al.* 1992). The estimated thickness of the elastic plate is probably related in both examples to the very young age of the oceanic lithosphere: the sections are only 70 and 110 km away from the spreading axis for the Orozco and Vema transform faults, respectively.

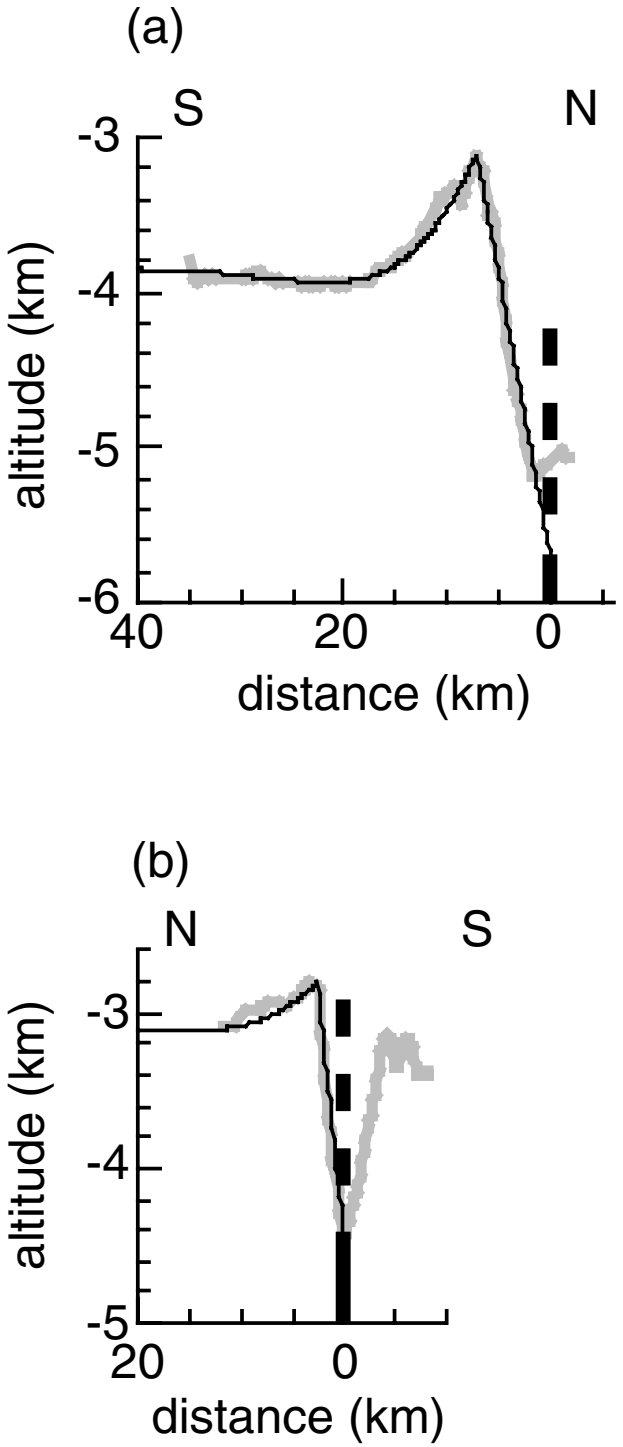

Figure 8. Modelling of the flexure of an elastic plate compared with the topography of oceanic transverse ridges. (a) Vema transform fault (topography from InterRidge Data Base); $h = 1.85$ km, $T_e = 1.5$ km, $s = 20°$. (b) Orozco transform faults (topography from Madsen *et al.* 1986); $h = 1.35$ km, $T_e = 1$ km, $s = 32°$. Both are below sea level. Same legend as in Fig. 6.

DISCUSSION

As shown by the examples presented above, erosion of the transform border is a mechanism that can, by itself, explain the uplift of a shoulder along the transform fault in intracontinental and

continent–ocean settings. However, this mechanism is based on the assumption that the transform fault is a stress-free boundary.

In intraoceanic setting, the coupling of the lithospheres across the transform fault may induce the downward flexure of the older oceanic plate, as suggested by Sandwell & Schubert (1982). However, this downward flexure is only observed in the inactive parts of the oceanic fracture zones, not along the active transform faults, suggesting that coupling may occur only when transform faults become inactive.

Along continent–ocean transform faults, the thermal subsidence of coupled lithospheres may also result in downward flexure of the continental lithosphere (Lorenzo & Wessel 1997), but the widespread occurrence of marginal ridges (upward flexure) along transform continental margins again suggests that the transform faults may be stress-free boundaries, at least in the active parts.

Finally, along intracontinental transform faults, thermal subsidence does not induce vertical displacements as for the oceanic lithosphere. Consequently, the coupling or uncoupling across the transform cannot be discussed on the basis of the topography.

We can also discuss the main limitation of the erosional model: the proposed model requires but does not explain the origin of the topographic step along the transform fault. In the case of transform continental margins, the continental crust lies against the oceanic crust, and the huge difference of crustal thicknesses on either side of the transform explains the difference of elevation.

In intracontinental and intraoceanic settings, the topographic step is not between two plates, but between a plate border and a transform valley. The origin of the transform valley is not clear: at oceanic transforms, it can be a strip of anomalously thin oceanic crust, emplaced at the ends of the oceanic accretion axis, where the magmatic accretion decreases (Cormier *et al.* 1984; Prince & Forsyth 1988; White *et al.* 1992); in an intracontinental transform such as the Dead Sea transform, the pull-apart basins indicate extension parallel to the transform (Garfunkel *et al.* 1981; Kashai & Croker 1987). These two explanations of the initial topographic step do not interact with the transform shoulder uplift generated by erosion.

Transtension (i.e. a small amount of divergence along the transform fault) can also explain the transform valley. If the transform fault is not vertical, the tectonic unloading caused by this extension may uplift the transform shoulder. If this last mechanism operates, then erosional unloading only explains an additional uplift along the transform fault, and the proportion of tectonic unloading versus erosional unloading increases as the dip of the transform fault decreases.

Finally, one can ask whether the erosional model excludes other hypotheses for the formation of transform shoulders?

In the example of the Dead Sea transform, the existence and amount of divergence is controversial, from pure strike-slip movement (Girdler 1990), to a small component of transverse extension (Garfunkel 1981), or oblique extension (Mart 1991). Wdowinski & Zilberman (1996) consider the transform fault as listric in cross-section (vertical at the surface, horizontal at depth), and accommodating 2–8 km of extension perpendicular to the transform axis. This extension creates a deep trough along the transform, but the tectonic unloading caused by crustal thinning is not able alone to explain the shoulder uplift. An 'additional unmodelled load' is required (Wdowinski & Zilberman 1996), which could be caused by erosion of the transform border (Figs 6a and b). If extension perpendicular to the Dead Sea transform exists, and if the transform fault is not vertical, then erosion of the transform border is only an additional mechanism that contributes to the shoulder uplift. In contrast, if the transform fault is vertical as it appears on upper crustal sections (Kashai & Croker 1987), then the crustal thinning west of the transform fault does not unload the eastern uplifted plate, and erosion can be the main cause of the transform shoulder uplift.

For continent–ocean transitions across a transform fault, the models of heat transfer (Todd & Keen 1989; Lorenzo & Vera 1992) assume local isostasy, and present the crustal thinning as a consequence of erosion above sea level. This mechanism cannot explain the permanent uplift below sea level, as observed along the marginal ridges of many transform continental margins. Moreover, Gadd & Scrutton (1997) showed that regional compensation drastically reduces the uplift owing to the heat transfer mechanism, and neither geological (Basile *et al.* 1998) nor geophysical data (Sage *et al.* 2000) show direct or indirect evidence for lateral heat transfer across the CIG transform margin at the time of ridge–transform intersection. As noted in the introduction, the step geometry is not realistic for transform topography, especially for large elevation differences as at transform margins. All of these arguments reject the model of lateral heat transfer for uplift of the transform continental margin, or at least reduce this mechanism to a second-order effect on the topography, either directly, or indirectly, by modifying the elastic thickness of the continental lithosphere and consequently modifying the shape and the amplitude of the flexure.

In intraoceanic transform faults, the erosional model only explains small relief features, or a small part of the uplift of transverse ridges. The erosional model does not improve the tectonic models of uplift (e.g. Pockalny *et al.* 1996), where the unloading is produced directly by normal faulting in response to changes in the spreading direction. In contrast, erosion can amplify an initial uplift driven by thermal mechanisms (Chen 1988), or at slow spreading axes, by the uplift of the oceanic rift shoulders. Moreover, erosion can make this uplift permanent, even when the initial mechanism is transient. This amplification is, however, probably too weak to explain the uplift of the main transverse ridges (Vema or Romanche) in the Atlantic Ocean. In any case, a full test of flexural uplift driven by erosion in intraoceanic setting will require us to investigate the temporal evolution from the transform-spreading axis intersection up to the inactive fracture zone.

CONCLUSIONS

In intracontinental and continental–oceanic settings, the model of flexural uplift driven by the erosion of a transform border correctly fits the morphology of transform fault shoulders. In these two geodynamic settings, this mechanism can be the main cause of transform uplift, rather than lateral heat transfer or extension perpendicular to the transform. In an intraoceanic setting, the uplift caused by erosion seems to be too weak to explain by itself the high-standing transverse ridges, but it can amplify a transient uplift related to another mechanism such as the uplift of the oceanic rift shoulders. Finally, erosion along transform faults is a ubiquitous phenomenon in all the successive geodynamic settings (intracontinental, continent–ocean, intraoceanic) experienced during the evolution of a given transform fault; a further development of the erosional model may include the time-dependent evolution of the environment (aerial or submarine), of the height submitted to erosion, and of the elastic thickness of the lithosphere.

ACKNOWLEDGMENTS

We thank P. Van der Beek for valuable comments and P. Clift for improvements to a previous version of the manuscript. We benefited

from constructive and useful reviews by J. Chen and R. Buck. CNRS-INSU (programme géosciences marines) partially funded this work.

REFERENCES

Basile, C., Mascle, J., Benkhelil, J. & Bouillin, J.P., 1998. Geodynamic evolution of the Côte d'Ivoire–Ghana transform margin: an overview from ODP Leg 159 results, in *Proc. ODP, Sci. Results,* Vol. 159, pp. 101–110, eds Mascle, J., Lohmann, G.P., Moullade, M., Ocean Driling Program, College Station, TX.

Basile, C., Mascle, J. Popoff, M. Bouillin, J.P. & Mascle, G., 1993. The Ivory Coast–Ghana transform margin: a marginal ridge structure deduced from seismic data, *Tectonophysics,* **222,** 1–19.

Bonatti, E., 1978. Vertical tectonism in oceanic fracture zones, *Earth planet. Sci. Lett.,* **37,** 369–379.

Bonatti, E., Ligi, M., Borsetti, A.M., Gasperini, L., Negri, A. & Sartori, R., 1996. Lower Cretaceous deposits trapped near the equatorial mid-Atlantic ridge, *Nature,* **380,** 518–520.

Burov, E.B. & Diament, M., 1995. The effective elastic thickness (T_e) of continental lithosphere: what does it really mean?, *J. geophys. Res.,* **100,** 3905–3927.

Chen, Y., 1988. Thermal model of oceanic transform faults, *J. geophys. Res.,* **93,** 8839–8851.

Chen, Y., 1989. A mechanical model for the inside corner uplift at a ridge–transform intersection, *J. geophys. Res.,* **97,** 9275–9282.

Clift, P.D. & Lorenzo, J.M., 1999. Flexural unloading and uplift along the Côte d'Ivoire–Ghana transform margin, equatorial Atlantic, *J. geophys. Res.,* **104,** 25 257–25 274.

Cormier, M.H., Detrick, R.S. & Purdy, G.M., 1984. Anomanously thin crust in oceanic fracture zones: new seismic constraints from the Kane fracture zone, *J. geophys. Res.,* **89,** 10 249–10 266.

Cronin, V.S., 1991. The cycloid relative-motion model and the kinematics of transform faulting, *Tectonophysics,* **187,** 215–249.

Gadd, S.A. & Scrutton, R.A., 1997. An integrated thermomechanical model for transform margin evolution, *Geo-Mar. Lett.,* **17,** 21–30.

Garfunkel, Z., 1981. Internal structure of the Dead Sea leaky transform (rift) in relation to plate kinematics, *Tectonophysics,* **80,** 81–108.

Garfunkel, Z., Zak, I. & Freund, R., 1981. Active faulting in the Dead Sea Rift, *Tectonophysics,* **80,** 1–26.

Girdler, R.W., 1990. The Dead Sea transform fault system, *Tectonophysics,* **180,** 1–13.

Honnorez, J., Villeneuve, M. & Mascle, J., 1994. Old continent-derived metasedimentary rocks in the equatorial Atlantic—an acoustic basement outcrop along the fossil trace of the Romanche transform fault at 6 degrees 30′W, *Mar. Geol.,* **117,** 237–251.

Kashai, E.L. & Croker, P.F., 1987. Structural geometry and evolution of the Dead Sea–Jordan rift system as deduced from new subsurface data, *Tectonophysics,* **141,** 33–60.

Lagabrielle, Y., Mamaloukas-Frangoulis, V., Cannat, M., Auzende, J.M., Honnorez, J., Mevel, C. & Bonatti, E., 1992. Vema fracture zone (central Atlantic): tectonic and magmatic evolution of the median ridge and the eastern ridge–transform intersection domain, *J. geophys. Res.,* **97,** 17 331–17 351.

Lorenzo, J.M. & Vera, E.E., 1992. Thermal uplift and erosion across the continent–ocean transform boundary of the southern Exmouth Plateau, *Earth planet. Sci. Lett.,* **108,** 79–92.

Lorenzo, J.M. & Wessel, P., 1997. Flexure across a continent–ocean fracture zone: the northern Falkland/Malvinas Plateau, South Atlantic, *Geo-Mar. Lett.,* **17,** 110–118.

Madsen, J.A., Fox, P.J. & Macdonald, K.C., 1986. Morphotectonic fabric of the Orozco transform fault: results from a sea beam investigation, *J. geophys. Res.,* **91,** 3439–3454.

Mart, Y., 1991. The Dead Sea Rift: from continental rift to incipient ocean, *Tectonophysics,* **197,** 155–179.

Mascle, J. *et al.*, 1996. *Proc. ODP, Initial Reports,* Vol. 159, Ocean Drilling Program, College Station, TX.

Pockalny, R.A., Gente, P. & Buck, R., 1996. Oceanic transverse ridges: a flexural response to fracture-zone-normal extension, *Geology,* **24,** 71–74.

Prince, R.A. & Forsyth, D.W., 1988. Horizontal extent of anomanously thin crust near the Vema Fracture zone from the three-dimension of gravity anomalies, *J. geophys. Res.,* **93,** 8051–8063.

Reid, I., 1989. Effects of lithospheric flow on the formation and evolution of a transform margin, *Earth planet. Sci. Lett.,* **95,** 38–52.

Sage, F., Basile, C., Mascle, J., Pontoise, B. & Whitmarsh, R.B., 2000. Crustal structure of the continent–ocean transition off the Côte d'Ivoire–Ghana transform margin: implications for thermal exchanges across the paleo-transform boundary, *Geophys. J. Int.,* **143,** 662–678.

Sandwell, D. & Schubert, G., 1982. Lithospheric flexure at fracture zones, *J. geophys. Res.,* **87,** 4657–4667.

Todd, B.J. & Keen, C.E., 1989. Temperature effects and their geological consequences at transform margins, *Can. J. Earth. Sci.,* **26,** 2591–2603.

Turcotte, D. & Schubert, G., 1982. *Geodynamics,* Wiley, New York.

Vågnes, E., 1997. Uplift at thermo-mechanically coupled ocean–continent transforms: modeled at the Senja fracture zone, southwestern Barents Sea, *Geo-Mar. Lett.,* **17,** 100–109.

Van Wees, J.D., 1994. Tectonics modeling of basin deformation and inversion dynamics, *PhD thesis,* Vrije Universiteit, Amsterdam.

Wdowinski, S. & Zilberman, E., 1996. Kinematic modelling of large–scale structural asymmetry across the Dead Sea Rift, *Tectonophysics,* **266,** 187–201.

Wdowinski, S. & Zilberman, E., 1997. Systematic analyses of the large-scale topography and structure across the Dead Sea Rift, *Tectonics,* **16,** 409–424.

White, R.S., McKenzie, D. & O'Nions, R.K., 1992. Oceanic crustal thickness from seismic measurements and rare Earth element inversions, *J. geophys. Res.,* **97,** 19 683–19 715.